



Cite this: *Green Chem.*, 2020, **22**, 8337

## Tuning the molar mass and substitution pattern of complex xylans from corn fibre using subcritical water extraction†

Reskandi C. Rudjito,<sup>a</sup> Amparo Jiménez-Quero,<sup>\*a</sup> Mahmoud Hamzaoui,<sup>b</sup> Stéphane Kohnen<sup>b</sup> and Francisco Vilaplana  <sup>a</sup>

Glucuronoarabinoxylan (GAX) is a structurally complex hemicellulose abundant in the cell wall of corn kernels that constitutes a valuable target for its valorisation from corn processing side streams. However, the crosslinked and recalcitrant nature of corn cell walls hinders its fractionation through mild green processes. In this study, we propose the extraction of GAX using subcritical water, where temperature, pH and time have been optimised to tune the extraction performance (yields and purity of the GAX) and the molecular structure of the extracted GAX (molar mass distribution, substitution pattern and presence of covalently bound phenolic moieties). Higher temperatures under unbuffered conditions caused a prominent drop in pH and autohydrolysis, resulting in a decrease of the molar mass ( $\sim 10^4$  Da) and the cleavage of arabinose substitutions. Mitigating the pH drop using mild buffered neutral and alkaline conditions provided higher molar masses of the extracted GAX ( $\sim 10^5$  Da), protecting as well the labile arabinose substitutions and resulting in a higher abundance of more complex glycan side chains. Subcritical water extraction preserved the phenolic acid moieties (mainly ferulic acid) covalently bound to polymeric GAX. Several forms of ferulic acid dehydrodimers (di-FA) were detected and identified by liquid chromatography–tandem mass spectrometry (HPLC–LC–MS<sup>2</sup>) and these di-FAs were particularly enriched in the mild alkaline extracts. We demonstrate that solely by carefully adjusting the operational parameters during subcritical water extraction we can tune the molar mass and complex substitutions of GAX, *i.e.* the degree and pattern of monomeric and oligomeric glycan side chains and ester-linked phenolic acid substitutions, without the use of additional catalysts. This molecular control over the production of corn GAX can invaluable benefit subsequent development of agroindustry-based biorefineries towards their conversion into novel bio-based materials for food and biomedical applications.

Received 25th August 2020,  
Accepted 2nd November 2020

DOI: 10.1039/d0gc02897e  
rsc.li/greenchem

## Introduction

Agricultural by-products are generated in vast amounts worldwide; some proceed into low-valued applications such as ingredients for feed, but for many, these biomasses are still underutilised today. A possible way to overcome this issue is to implement a biorefinery concept, in which residual biomass is reformed into industrially valuable goods by innovative means of sustainable processes.<sup>1</sup> An example of a residual biomass that potentially holds an assortment of applications is corn fibre (or corn bran) obtained from corn processing, such as

wet-milling. Corn itself is extensively produced worldwide, at more than 1100 million tonnes annually.<sup>2</sup> The corn fibre consists of the pericarp, aleurone, tip and remaining endosperm portion of the corn kernel.<sup>3–5</sup> In relative amounts, corn fibre is composed of 30–50% glucuronoarabinoxylan (GAX), 15–20% cellulose, 10–25% starch,<sup>6,7</sup> 8–12% protein,<sup>8</sup> 1.9% lipids, 0.7% lignin and 0.6% ash.<sup>6</sup> Small amounts of mixed-linked  $\beta$ -D-glucans are also present (0.8–1.7% of the whole grain).<sup>9</sup> Corn fibre has therefore a rich content of hemicelluloses and particularly GAX (Fig. 1a), which renders it a target biopolymer for the development of biorefinery processes for its isolation and conversion into valuable products for material, food and biomedical applications.

Corn GAX is one of the most complex plant polysaccharides as it is extensively decorated with variations of both monomeric and oligomeric substitutions. The core structure of GAX is composed of a (1  $\rightarrow$  4)-linked- $\beta$ -D-xylopyranosyl (Xyl) backbone with substitutions of  $\alpha$ -L-arabinofuranose (Ara) at the

<sup>a</sup>Division of Glycoscience, Department of Chemistry, School of Engineering Sciences in Chemistry, Biotechnology and Health, Royal Institute of Technology, Stockholm, Sweden. E-mail: [amparoq@kth.se](mailto:amparoq@kth.se), [franvila@kth.se](mailto:franvila@kth.se)

<sup>b</sup>Biomass Valorisation – Extraction, CELABOR, Chaineux, Belgium

† Electronic supplementary information (ESI) available. See DOI: [10.1039/d0gc02897e](https://doi.org/10.1039/d0gc02897e)



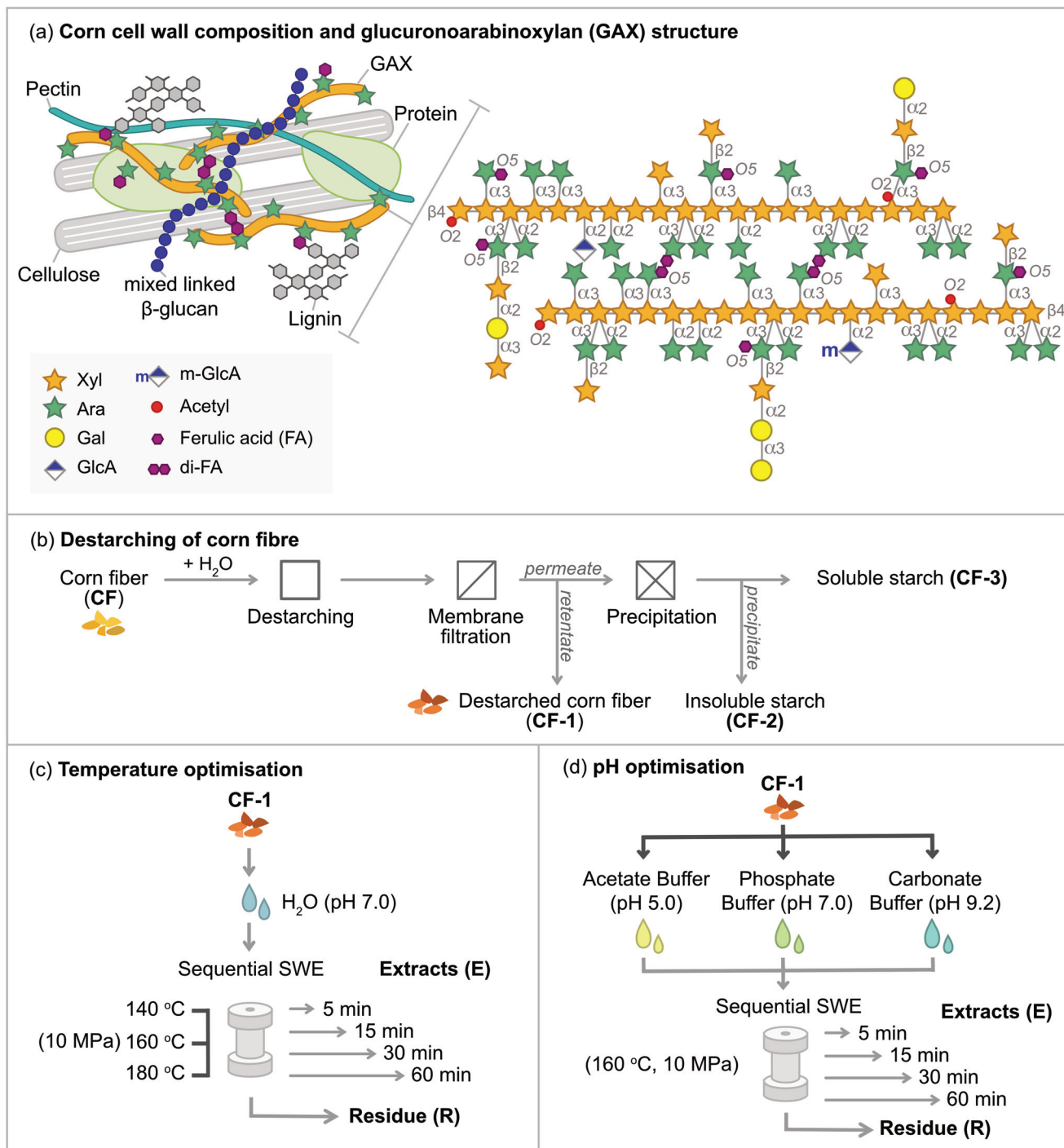


**Fig. 1** (a) Cell wall composition of corn fibre and proposed structure of glucuronoarabinoxylan (GAX).<sup>8,10–12,18,19</sup> Note: di-FA refers to ferulic acid dehydrodimer and m-GlcA refers to 4-O-methyl-d-glucuronic acid. Schematic overview of (b) destarching of corn fibre, (c) temperature optimisation and (d) pH optimisation in the SWE.

C(O)-3 and/or the C(O)-2 positions. In contrast with other relevant cereal arabinoxylans, oligomeric sidechains occur in corn cell walls as an extension of the arabinose substitutions, which can be further linked to xylose (Xyl) and galactose (Gal). The term glucurono- in GAX comes from the presence of  $\alpha$ -D-glucuronic acid (GlcA) at the C(O)-2 position. These acids can also

be present in their derivative form of 4-O-methyl-d-glucuronic acid (m-GlcA). Additionally, corn GAX is esterified to acetyl and phenolic groups, the latter primarily being ferulic acid (FA).<sup>10–13</sup> The content of ferulic acid in corn is strikingly high as compared to other cereal grains,<sup>14</sup> and its content in the pericarp is considered highest among other plant tissues.<sup>15</sup>



The amount of ferulic acid esterified to the GAX accounts for up to 4% of the dry matter.<sup>16</sup> A majority of this ferulic moiety is present in the monomeric form, while a minor extent is in the dehydromer form (di-FA) with 8-5', 5-5', 8-8' and 8-O-4' ferulic acid dehydromers being the most abundant.<sup>13</sup> These dehydromers are presumably the nodes that sustain the crosslinking of GAX to other GAX chains, lignin and protein in the cell wall matrix of corn fibre, and thus contributing significantly to its recalcitrance.<sup>6,17,18</sup>

The intricate and heterogeneous molecular structure of corn GAX along with its high phenolic content provides large versatility for their potential use in multifunctional applications. For instance, in the food and health sector, GAX is considered to be an important prebiotic for the modulation of the gut microbiota.<sup>20</sup> GAX has been reported to promote growth of butyrogenic bacteria, in which the butyrate produced from the anaerobic fermentation of GAX can have health benefits, such as improved gut barrier function and anticancer properties.<sup>21,22</sup> The ferulic acid component also exhibit anti-oxidant properties both in their free and bound form, as well as anti-inflammatory responses linked to a decreased risk of diabetes type 2.<sup>23</sup> In terms of material applications, the cross-linking ability of GAX due to the presence of phenolic acids, has been capitalized for the development of hydrogels,<sup>24,25</sup> which can be implemented for drug delivery, encapsulation of cells as well as food gels and texturizing agents.<sup>26,27</sup>

Such applications drive the importance to extract and fractionate GAX with desirable structural properties, in a manner that is both commercially feasible and environmentally sustainable. Nonetheless, the isolation of GAX, or xylans in general, from lignocellulosic biomass is not easy. Xylans, together with other biomacromolecules intertwine and form a cross-linked matrix in plant cell walls. Relatively harsh conditions are required to disrupt the non-covalent and covalent bonds present in these cell walls, enabling the release of their individual components. Conventional methods of extracting xylans from cereal biomass involve the use of strong alkaline solutions,<sup>28,29</sup> which disrupt supramolecular interactions (e.g. hydrogen bonds) between xylans and cellulose, as well as cleave ester bonds that are responsible for intermolecular cross-linking.<sup>30</sup> Acidic conditions are likewise used for extraction, but they result in substantial degradation and are therefore mainly used for the recovery of monosaccharides.<sup>31,32</sup> In either case, the use of concentrated alkaline or acidic solutions require rigorous downstream processing, which is not only costly but also unsustainable in terms of the resources and energy used.

An alternative approach to extract GAX is to use water-based extractions, such as subcritical water extraction (SWE) that allows for relatively quick extraction procedures and minimised downstream processing of the extract. The use of water is environmentally friendly, as it is non-toxic, widely available, and can be repeatedly recycled. In subcritical conditions, water becomes more compressible due to a decrease in density,<sup>33</sup> dielectric strength, polarity,<sup>34</sup> and viscosity also decreases,<sup>35</sup> which enhances its penetration and diffusivity into the

biomass. The physical changes that occur in subcritical conditions transforms water into an effective media for extraction, reducing or even omitting the need for additional catalysts. In previous works we have demonstrated the feasibility of subcritical water combined with enzymatic treatments to selectively fractionate different polysaccharide populations from various cereal brans with high yields and purities, preserving their bioactive (antioxidant) functionalities.<sup>36,37</sup> In this study, we demonstrate that solely controlling the operational conditions during subcritical water extraction (temperature, time, and pH), we can effectively modulate the molecular structure of corn GAX in terms of molar mass, pattern and complexity of side chain substitutions, as well as the amount and diversity of phenolic moieties. This molecular control enables the extraction and fractionation of corn GAX with targeted molecular features, which will benefit further chemo-enzymatic tailoring and macroscopic properties towards their application in advanced material and biomedical applications.

## Experimental

### Bioprocess design

**Biomass and reagents.** Corn fibre was provided by Cargill Deutschland GmbH (Krefeld, Germany). The 5,5' and the 8-8' ferulic acid dehydromers were kindly gifted by Prof. Florent Allais and Amandine Léa Flourat (AgroParisTech, Pomacle, France). Chemicals used in the study were of analytical grade and purchased from Sigma-Aldrich (Sigma-Aldrich, Stockholm, Sweden), unless otherwise stated.

**Destarching pre-treatment.** In brief, 500 g of fresh corn fibre (CF-0) was mixed in 2.5 L of water (bath ratio 1 : 5) for 4 hours at 80 °C. After filtration through a Whatman filter paper (pore size of 25 µm), the destarched corn fibre (CF-1) was freeze-dried and the supernatant was stored at 4 °C for 2 days to precipitate insoluble starch (CF-2). After centrifugation, both fractions of insoluble starch (CF-2) and soluble starch (CF-3) were separated and freeze dried. CF-1 was further grinded using a kitchen grinder (OBH Nordica, Stockholm, Sweden) to a particle size of 0.5–1.5 mm. All the resulting fractions (CF-0, CF-1, CF-2, CF-3) were stored at –20 °C until further analysis. The destarching process is shown in Fig. 1b, while the fractionation yields and composition are shown in ESI Tables S1 and S2,† respectively. Starch-rich fractions were further characterised in terms of molar mass distributions and branch-chain length by size-exclusion chromatography (see ESI†).

**Subcritical water extraction of GAX.** Subcritical water extraction (SWE) was performed using Accelerated Solvent Extraction Dionex™ ASE™ 350 (Thermo Fisher Scientific Inc., USA), as previously described,<sup>38</sup> with modifications. Briefly, 3 g of destarched corn fibre (CF-1) was loaded into an extraction cell prepped with Dionex ASE Prep DE Diatomaceous Earth (Thermo Fisher Scientific, Stockholm, Sweden) lined in between ASE Extraction Cellulose Filters (Thermo Fisher Scientific, Stockholm, Sweden). For temperature optimisation, CF-1 was sequentially extracted under static mode using MilliQ



$\text{H}_2\text{O}$  (pH initially adjusted to 7.0) at different temperatures (140 °C, 160 °C, 180 °C) for 5, 15, 30 and 60 min, respectively. Dialysis was not performed on these extracts and they were directly freeze-dried. For pH optimisation, 3 g of CF-1 was subjected to SWE using different buffer solutions (100 mM acetate buffer pH 5, 100 mM phosphate buffer pH 7 and 100 mM carbonate buffer pH 9.2) at 160 °C for 5, 15, 30 and 60 min, respectively. The pH optimised extracts were dialysed against deionised water using 3.5 kDa MWCO Spectra/Por membranes (Spectrum Laboratories Inc., Rancho Dominguez, CA, USA) for 72 h and subsequently freeze-dried. During extraction, the extractor retained a pressure of 10–11 MPa and a solid to liquid ratio of 1:14 (w/v). The extraction was performed in duplicates for each of the conditions. A schematic figure of the SWE performed in this study is shown in Fig. 1c and d. The weight of the dry extracts was then used to determine the extraction yields on a dry weight basis. Humidity of CF-1 was determined as the gravimetric difference before after freeze-drying for 72 h (quadruplicate).

### Characterisation of corn fibre fractions

**Monosaccharide composition.** The monosaccharide analysis was determined using the Dionex CarboPac PA1 column on the ICS3000 system (Dionex, Sunnyvale, CA, USA) after acidic methanolysis on the extracts<sup>39</sup> and sulfuric hydrolysis on the destarched corn fibre (CF-1) and residues.<sup>40</sup> Briefly for the extracts, 1 mg of sample (triplicate) was mixed with 1 ml of 2 M HCl in MeOH and flushed with argon. Methanolysis was performed for 5 h at 100 °C. Samples were neutralised with pyridine (approx. 200 µl), cooled and dried to room temperature under compressed air. Dried samples were then hydrolysed with 1 ml of 2 M TFA for 1 h at 120 °C, dried and resuspended in MilliQ  $\text{H}_2\text{O}$ . For the CF-1 and residues, 4 mg of sample (triplicate) was hydrolysed in two-steps: first with 72%  $\text{H}_2\text{SO}_4$  (125 µl) for 1 h at room temperature and second with 1 M  $\text{H}_2\text{SO}_4$  (1375 µl of  $\text{H}_2\text{O}$  was added) for 3 h at 100 °C. Hydrolysed samples of both methods were filtered through a Chromacol 0.2 µm filter (Thermo Scientific, Stockholm, Sweden), diluted with MilliQ  $\text{H}_2\text{O}$  and analysed on the ICS3000, as previously described.<sup>41</sup> The monosaccharide content was calculated in reference to a standard mixture (0.005–0.01 mg ml<sup>−1</sup>) containing Fuc, Rha, Ara, Xyl, Gal, Glc, Man, GalA, GlcA and m-GlcA (Carbosynth Ltd, Berkshire, UK).

**Total starch content.** The total starch content was quantified in triplicate using the K-TSTA-50A Total Starch kit (Megazyme, Wicklow, Ireland). The branch-chain length distributions of the starch-rich fractions were analysed by enzymatic debranching and subsequent analysis of the linear starch branches by size exclusion chromatography (see ESI†).<sup>42</sup>

**Ester-linked phenolic acid content.** The ester-linked phenolic acid was released through saponification followed by analysis using HPLC.<sup>43,44</sup> In duplicate, 10 mg of sample was weighed into amber microcentrifuge tubes (Eppendorf, Hamburg, Germany) and mixed with 500 µl of 2 M NaOH. Samples were flushed with nitrogen and saponified under agitation for 17 h at 30 °C. The saponified solution was adjusted

to pH 3.0 using 12 M HCl. Ethyl acetate was then added (2:1, v/v) to extract the released phenolic acids. Partition was performed 3 times and the pulled ethyl acetate fraction was dried under a nitrogen stream. Dried samples were resuspended in methanol: 2% acetic acid (1:1, v/v) and analysed using a ZORBAX StableBond C18 column (Agilent Technologies, Santa Clara, CA, USA) fitted to a Waters 2695 separation module (Waters Corporation, Milford, MA, USA) coupled to a photo-diode array detector (Waters Corporation, Milford, MA, USA) at 200–400 nm. The mobile phase consisted of 2% acetic acid in  $\text{H}_2\text{O}$  (v/v) (eluent A) and 100% methanol (eluent B). The gradient was as follows: 100–75% A (11 min), 71.25% A (4 min), 64% A (10 min), 55% A (10 min), 35% A (3 min), 100% A (3 min) and 100% A (4 min). The column was washed with 100% B for 10 min and equilibrated to the initial condition for 5 min before the next injection. The phenolic acid content was quantified in reference to external standards of caffeic acid, *p*-coumaric acid, *trans*-ferulic acid, sinapic-acid, *trans*-cinnamic acid, 8-8' di-FA and 5-5' di-FA (0.005–0.1 mg ml<sup>−1</sup>).

**HPLC-ESI-MS<sup>2</sup> analysis of ferulic acid dehydrodimers.** Identification of unknown ferulic acid dehydrodimers was performed using a HPLC system coupled to an electrospray ionisation mass spectrometry ESI-MS using a Synapt G2 mass spectrometer (Waters Corporation, Milford, MA, USA) in positive mode. Capillary and cone voltage were set to 3 kV and 10 kV, respectively. Separation was achieved using an Eclipse Plus C18 column (Agilent Technologies, Santa Clara, CA, USA). The mobile phase consisted of 0.1% (v/v) formic acid in  $\text{H}_2\text{O}$  (eluent A) and 0.1% (v/v) formic acid in acetonitrile (eluent B). The gradient was as follows: 95% A (2 min), 62% A (15 min), 10% A (3 min), 10% A (1 min), 95% A (5 min) and 95% A (1 min). The retention times of the ferulic acid dehydrodimers were referenced using an external standard mixture containing monomeric ferulic acid, 5-5' di-FA and 8-8' di-FA at 0.05 mg ml<sup>−1</sup>. MS<sup>2</sup> analysis was performed in positive mode using ion collision induced dissociation (CID) with nitrogen as collision gas. Fragmentation was achieved by selecting the 369.1 *m/z* ion and subjecting it to a collision energy of 20 eV. Analysis of chromatograms and spectra was performed using the MassLynx software (Waters Corporation, Milford, MA, USA).

**Ester-linked acetic acid content.** The quantification of ester-linked acetic acid was performed by saponification and HPLC as previously described.<sup>45</sup> In short, 7 mg of sample (duplicate) was mixed with 300 µl of  $\text{H}_2\text{O}$  and saponified using 1.2 ml of 0.8 M NaOH for 17 h at 60 °C. Propionic acid 1 M (10 µl) was added as an internal standard. Saponified samples were neutralised using 12 M HCl and filtered through Chromacol 0.2 µm filters. Separation was achieved using a Rezex organic acid column (Phenomenex, Torrance, CA, USA) fitted to the Ultimate-3000 HPLC system (Dionex, Sunnyvale, CA, USA) coupled to a UV detector (210 nm). An isocratic flow of 2.5 mM  $\text{H}_2\text{SO}_4$  at 0.5 ml min<sup>−1</sup> (50 °C) was used in the HPLC.

**Protein content.** Protein content of soluble samples, *i.e.* extracts, were determined using the Bradford method in triplicate.<sup>46</sup> The Protein Assay Dye Reagent Concentrate was purchased from Bio-rad (Stockholm, Sweden).



**Molar mass distributions.** The molar mass distributions were determined using the SECurity 1260 size exclusion chromatography (Polymer Standard Services, Mainz, Germany) coupled to a refractive index, as previously described.<sup>36</sup>

**DPPH radical scavenging activity.** The radical scavenging activity was measured using 2,2-diphenyl-1-picrylhydrazyl (DPPH),<sup>47</sup> with modifications. Briefly, 100  $\mu$ l of extract solution (0.1–5 mg ml<sup>-1</sup>) was pipetted into a 96-well microtiter plate in duplicate. To that, 100  $\mu$ l of 0.2 mM of DPPH in methanol was added into the sample and the microtiter plate was incubated at room temperature in the dark for 30 min. The loss of colour due to radical scavenging activity was analysed using the Clariostar microplate reader (BMG Labtech, Ortenberg, Germany) at 517 nm. A standard curve was constructed using the DPPH solution (1–100  $\mu$ M) and the radical scavenging activity was measured and evaluated by comparison with the activity of *trans*-ferulic acid and ascorbic acid standards.

**Glycosidic linkage analysis.** The analysis was performed by per-*O*-methylation of the polysaccharidic sample, followed by hydrolysis, derivatisation and analysis using GC-MS, as formerly described.<sup>48</sup> In triplicate, 1 mg of sample was dissolved in 400  $\mu$ l DMSO, flushed with argon and kept stirring for 17 h at room temperature. Dissolved samples were mixed with 200 mg of freshly ground NaOH, followed by 30  $\mu$ l of CH<sub>3</sub>I, which was added 5 times at 10 min intervals. Each addition of CH<sub>3</sub>I was proceeded with argon flushing and either stirring (3 times) or sonication (2 times). Methylated polysaccharides were partitioned using DCM : H<sub>2</sub>O (1 : 2, v/v). H<sub>2</sub>O was removed and again added (3 times). Pulled methylated polysaccharides in the DCM fraction was dried and hydrolysed with 1 ml of 2 M TFA for 3 h at 121 °C. The hydrolysate was then dried and reduced with 1 M NaBD<sub>4</sub> in NH<sub>3</sub> for 1.5 h at room temperature. Reduced samples were neutralised with 10% (v/v) HAc in MeOH 3 times and derivatised using pyridine : acetic anhydride (1 : 1 v/v, 200  $\mu$ l) for 1 h at 100 °C. Partially methylated alditol acetates (PMAAs) were separated on the SPTM 2380 capillary column (Supelco, St Louis, MO, USA) fitted to the HP-6890 gas chromatographer (Agilent Technologies, Santa Clara, CA, USA) coupled to the HP-5973 electron impact mass spectrometer (Agilent Technologies, Santa Clara, CA, USA). Separation was achieved using the method previously described.<sup>38</sup>

## Results and discussion

### Steeping process removes starch from corn fibre – a prerequisite for SWE

Destarching of the corn fibre by aqueous steeping was implemented prior to subcritical water extraction (SWE), in order to isolate the interfering starch in polymeric form and to prevent possible clogging of the extraction system.<sup>38</sup> The yields, monosaccharide composition and starch content of the different fractions during the steeping destarching process were analysed (ESI Tables S1 and S2†). The steeping process proved to be successful since the treated corn fibre after fil-

tration (CF-1) showed a decrease in the total glucose content and an almost negligible starch content below 1.5%. The destarched corn fibre also resulted in an increase in the glucuronoxylans (GAX) purity to 63.8%, which constitutes a promising starting material for the implementation of SWE. The insoluble starch fraction after cold precipitation (CF-2) showed a relatively low carbohydrate and starch purity, which could be due to the removal of protein and other components from the corn fibre. The soluble fraction (CF-3) is, on the other hand, markedly enriched in starch, which again evidences the viability of the process. Some residual pectin and xylan content can be observed as well, which correspond to solubilised populations during the steeping conditions.

The molecular structure of the soluble and insoluble starch fractions obtained from the steeping pre-treatment was characterised by size exclusion chromatography (ESI Fig. S1†), showing the typical bimodal distribution corresponding to the amylopectin ( $M_w \sim 10^7$  Da) and amylose populations ( $M_w \sim 10^6$  Da). The chain length distributions of the branches verified the differences observed for the insoluble and soluble starch samples. The insoluble starch showed a higher abundance of the peak corresponding to the amylose long branches (DP  $\sim$  100–10 000), whereas the amylopectin shorter branches (DP  $\sim$  10–100) were the main component of the soluble starch fraction. On the other hand, the crystalline structure of the corn fibre fractions was analysed using X-ray diffraction (ESI Fig. S2†). The original corn fibre (CF-0) and the destarched corn fibre (CF-1) showed intense peaks at the scattering angles of 15–25°, which can be attributed to the presence of cellulose with low crystallinity. The starch samples did not exhibit the typical scattering signals for semi-crystalline starch, which indicate that the supramolecular organization of the starch chains has been lost during the steeping process and undergone gelatinization. The recovered starch fractions can be developed into different applications, for instance it can be derivatised (*e.g.* by esterification) to generate various biopolymeric matrices<sup>49</sup> and further compatibilized to produce bio-based blends and composites.<sup>50</sup>

### Higher temperature during SWE promotes higher yields and purity of GAX but induces autohydrolysis

In the SWE, we first investigated the effect of temperature (140 °C, 160 °C, 180 °C) on the extraction of GAX from destarched corn fibre (CF-1). The total solid yields (pulled extracts and residue) and yields of extracts at different extraction times are shown in Fig. 2a and b, respectively. It is apparent that the increase of temperature resulted in higher extraction yields and consequently lower residual yields. As extraction time increased, so did the extraction yields (Fig. 2b), with the exception at 180 °C. Here, the extraction yield was highest at 15 min, inferring that at higher temperatures the maximum total yield can be achieved at earlier times. The extraction of polysaccharides in the SWE is governed by a combination of events, *i.e.* direct solubilization and detachment from the biomass network as well as hydrolytic events that may occur at



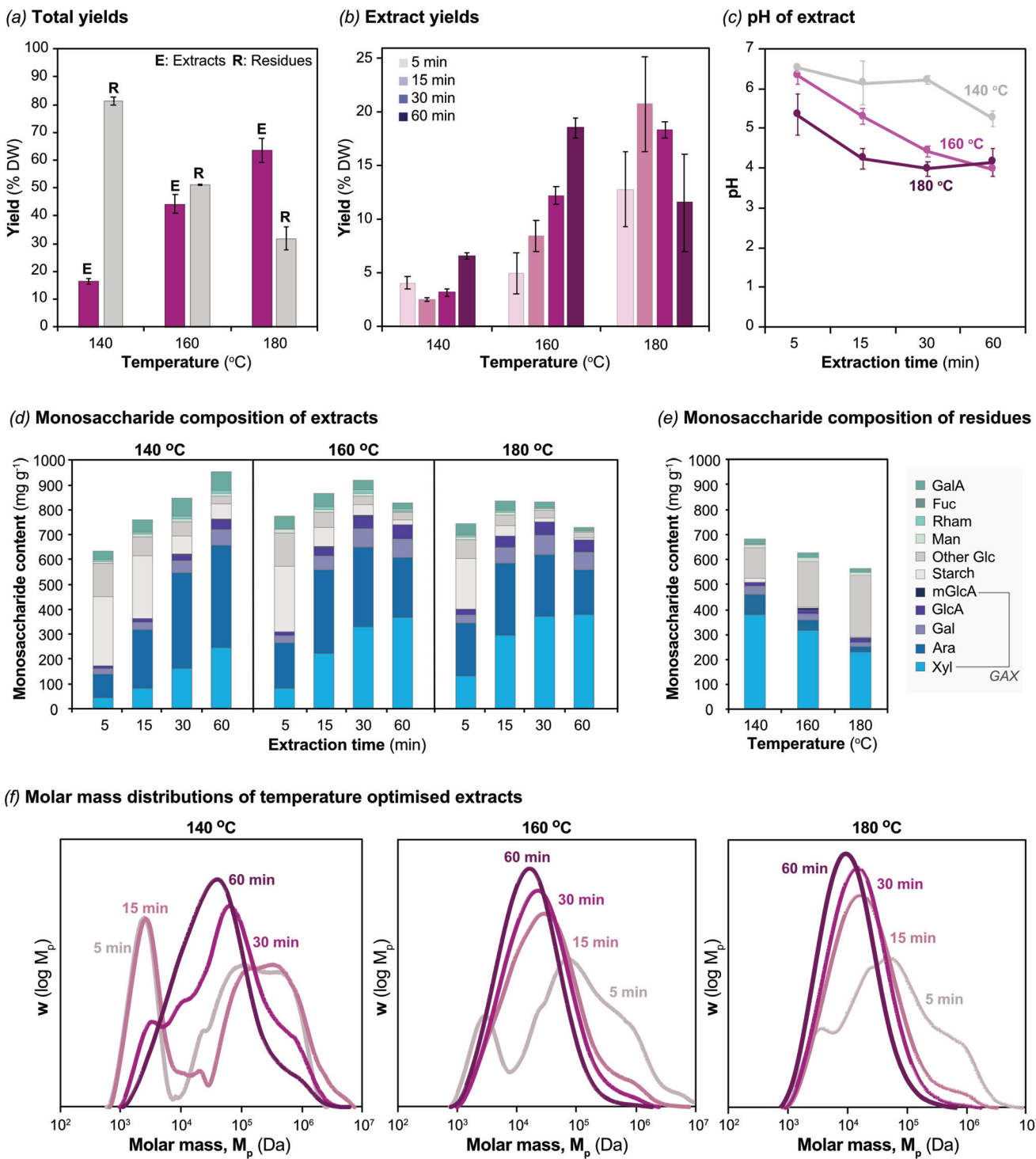


**Fig. 2** (a) Total solid yields and (b) extract yields from temperature optimisation of SWE. Yields are calculated in terms of percentage dry weight (% DW). (c) The pH of the extracts. Monosaccharide composition of extracts (d) and residues (e) are shown in terms of mg per gram of dry sample. The glucuronoarabinoxylan (GAX) content is estimated by the composition of xylose (Xyl), arabinose (Ara), galactose (Gal), glucuronic acid (GlcA) and 4-O-D-methyl glucuronic acid (mGlcA). (f) Molar mass distributions of temperature optimised extracts.

high temperatures, whereby both are followed by diffusion out of the biomass and dissolution into the extraction media.<sup>51-53</sup> This, along with an improved mass transfer at subcritical condition explained the increase of extract yield as a function of

both temperature and time. Additionally, deviations were observed in the extraction yields, particularly at 180 °C, which are likely attributed to the heterogenous nature of the corn fibre.



During extraction, the pH of the extracts also decreased (Fig. 2c) and this is an effect of the subcritical conditions<sup>54</sup> as well as deacetylation.<sup>55,56</sup> Release of acetyl groups is positively affected by temperature<sup>57,58</sup> and this is well reflected in the faster drop of pH at 180 °C as compared to 160 °C or 140 °C (initial pH of water was 7.0). The acidification of water is often linked to an increase in the extraction rate, as acid groups catalyse cleavage and subsequent dissolution of polysaccharides, *i.e.* autohydrolysis.<sup>59</sup>

In terms of the monosaccharide composition (Fig. 2d), the dominating polysaccharides present in the extracts were glucans and GAX, in which the latter is presumably composed of xylose (Xyl), arabinose (Ara), galactose (Gal), glucuronic acid (GlcA) and 4-O-methyl-D-glucuronic acid (mGlcA).<sup>6,8,10,11</sup> The glucans originate from either residual starch of the endosperm or mixed-linked  $\beta$ -glucans that are present in low amounts.<sup>9</sup> These two dominating polysaccharide populations, *i.e.* the glucans and GAX, underwent a shift in abundance with time; as the glucan population decreased, the GAX population increased. This shift was clearly observed at all temperatures. At 140 °C, however, the shift seemed to occur more slowly than at 160 °C and 180 °C, where GAX-rich extracts (GAX content > 80%) were only shown after 60 min of extraction. The recovery of glucans prior to GAX suggests that glucans were more extractable than GAX in the SWE, corresponding well to previous studies highlighting the recalcitrance of corn GAX.<sup>60–63</sup> Furthermore, the monosaccharide composition of the residues similarly showed glucans and GAX as the two main polysaccharides that remain in the corn fibre after SWE (Fig. 2e). The glucans in the residues, however, most likely corresponded to cellulose, which is less susceptible to extraction in the SWE. Lower amounts of other sugars, such as galacturonic acid (GalA) and mannose (Man) were also detected in both the extracts and residues (Fig. 2d), and these can originate from less abundant polysaccharides such as pectins and mannan, as shown by linkage analysis (ESI Tables S7 and S8†). Aside from the carbohydrate portion of the extracts, low amounts of proteins were also extracted in the SWE (ESI Table S4†). The extracted proteins can potentially be both storage proteins (*e.g.* zein) that are associated with starch in the endosperm<sup>64,65</sup> and structural proteins such as extensin and arabinogalactan proteins (ESI Fig. S3†) that can associate with the GAX.<sup>10,66</sup>

In addition to changes in the yield and purity of the extracts, temperature also greatly modulated the molar mass of the GAX *via* autohydrolysis. The observable drop in pH, which resulted in backbone cleavage, was clearly seen at 160 °C (15–60 min) and 180 °C (15–60 min), where a majority of the GAX were approximately 10<sup>4</sup> Da in length (Fig. 2f). As the extraction time increased, the molar mass distributions shifted more to lower molar masses. This shift was expectedly more evident at 180 °C as the  $\bar{M}_w$  value dropped from 61.7 kDa at 15 min to 18.9 kDa at 60 min (Table 1). Maintaining a high molar mass is often preferred when the application is material oriented. Thus, to accommodate a high molar mass as well as sufficient yields and purity, we have opted for 160 °C as the chosen temperature for subsequent pH optimisation.

## Buffered pH conditions during SWE mitigate autohydrolysis and influence the total yields and the molar mass of extracted corn GAX

In the second part of the SWE optimisation, we investigated the effect of pH on the extraction of GAX under a single temperature condition, *i.e.* at 160 °C. The total solid yields and extract yields are shown in Fig. 3a and b, respectively. A difference between the temperature optimised extracts is that here the extracts were dialysed to remove the salts from the buffer. As a result, the yields correspond to only polymeric forms of the extracted biomacromolecules that remained after dialysis. The results showed that mild alkaline conditions favoured the extraction, resulting in the highest yield. Extraction yields at pH 9.2 were particularly high at 30 and 60 min, and this could be explained by the rupture of ester bonds sustaining GAX cross-linking to other GAX chains, protein and lignin.<sup>6,17,18</sup> In contrast, the lowest yield was obtained at pH 5.0. At mild acidic conditions, autohydrolysis most likely also occurred, resulting in the accumulation of shorter oligosaccharides that would have been easily washed out during dialysis. In respect to the mass balances, the mass loss was highest at pH 5.0 (24.5%), while at pH 7.0 and pH 9.2, the mass loss during dialysis was noticeably less at 15.1% and 6.8%, respectively (Fig. 3a). Taking into consideration that the mass lost was essentially part of the extraction yield, the sum of the solid yield (yield measured + mass lost) at pH 5.0 was in fact higher than at pH 7.0. This suggests that in terms of yield alone, maintaining a neutral pH in the SWE does not benefit the extraction of GAX from corn fibre in comparison to acidified or alkaline conditions, as opposed to what we observed previously for wheat bran.<sup>36</sup>

The pH of the extracts, as shown in Fig. 3c, was generally maintained in accordance to the buffer conditions used. A slight drop in pH was observed in the 5 min extract of pH 9.2 and this could be caused by a substantial release of acetic groups. In respect to the acetyl content, which was measured after dialysis, a low amount was measured at pH 9.2 (ESI Table S5†). A majority of the acetic groups, which would be unbound as a result of saponification, would have likely been washed out during dialysis. In contrast, at pH 5.0, the acetic acid moieties remained on the GAX and its content increased with increasing GAX content.

The monosaccharide composition of the pH-optimised extracts showed a comparable trend to that of the temperature-optimised extracts; with time, the amount of GAX increased while the glucans decreased (Fig. 3d). The shift from a glucan-rich to a GAX-rich extract was fairly slow at both pH 5.0 and pH 7.0, whereby at pH 7.0, a GAX content of 87.3% was only reached after 60 min. In contrast, at pH 9.2, a GAX content of 92.4% was already reached at 30 min. The sharp increase in yield at 30 and 60 min indicated that the optimum condition for the extraction of GAX at pH 9.2 had been reached. Such high purities of GAX obtained at pH 9.2 implies that indeed the use of alkaline conditions, even in combination with SWE technology, is still most selective for the extraction of hemicel-

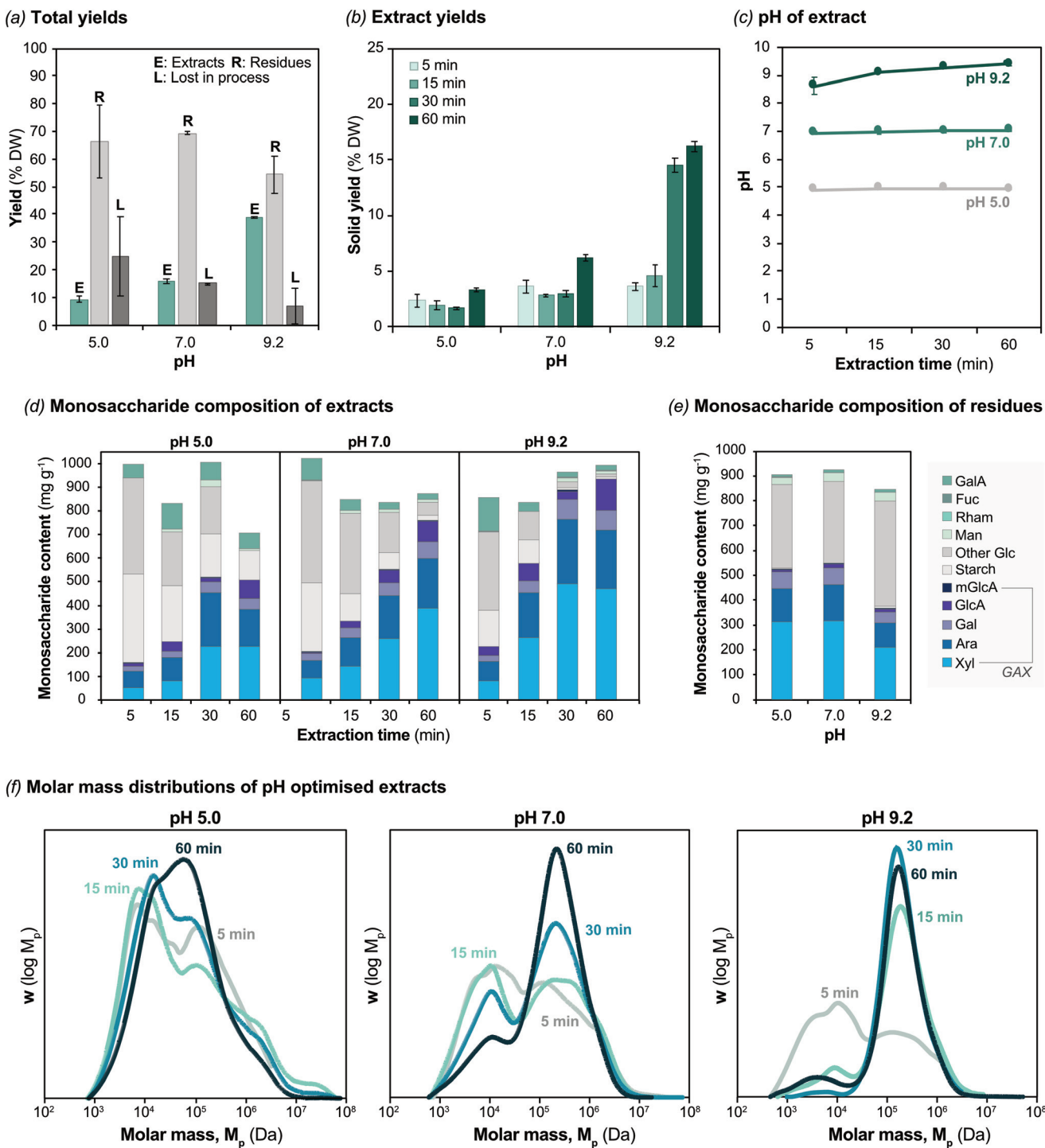




Table 1 Molecular characterisation of the extracted GAX from the temperature and pH optimisation in the SWE

	Temperature optimisation										pH optimisation						
	160 °C					180 °C					pH 7.0			pH 9.2			
	5'	15'	30'	60'	5'	15'	30'	60'	5'	15'	30'	60'	5'	15'	30'	60'	
Substitution pattern of the GAX from glycosidic linkage analysis																	
GAX <sup>a</sup> (mg g <sup>-1</sup> )	310.2	651.3	778.1	741.1	402.7	695.4	752.0	680.7	206.6	330.3	545.5	751.0	221.6	573.6	888.7	924.4	
Arabinose <sup>b</sup> (% mol)	TS <sup>e</sup>	31.5	22.6	18.8	13.2	19.1	13.4	8.7	3.4	27.7	24.7	24.8	17.2	30.3	23.0	20.0	
t-Arap	TS	5.5	7.8	3.9	3.3	4.6	3.6	2.9	0.5	0.6	0.6	0.3	0.4	0.3	1.0	0.3	
2-Arap	OS	5.8	6.7	7.5	7.9	8.7	9.0	9.2	2.9	3.0	3.3	4.6	3.3	4.7	5.6	5.1	
3-Araf	OS	5.7	5.8	6.0	5.1	6.7	6.7	6.2	2.1	1.1	1.3	3.6	2.0	3.6	2.4	5.2	
3-Araf/3Xylp	OS	3.2	3.8	3.3	2.0	5.8	4.1	3.4	3.5	0.0	0.0	0.0	0.0	0.0	0.0	0.0	
t-Xylp	TS	3.6	6.3	9.1	10.8	5.0	7.2	8.5	6.2	4.5	12.2	15.4	12.4	3.2	9.8	20.9	
2-Xylp/2-Arap	OS	0.1	0.1	0.1	0.1	0.0	0.0	0.1	0.0	0.0	0.0	0.0	0.0	0.0	0.0	0.0	
4-Xylp	BB, OS	10.3	13.6	17.3	22.8	14.7	19.3	23.5	30.1	18.0	10.0	8.9	10.6	12.4	9.8	8.1	
2,4-Xylp	BB	7.3	7.0	6.1	6.5	7.7	7.4	7.6	8.4	6.2	6.0	6.8	6.4	6.2	5.2	5.4	
3,4-Xylp	BB	9.4	9.5	10.7	11.5	11.7	11.8	12.8	15.3	15.8	16.9	16.2	16.1	13.2	15.4	14.9	
2,3,4-Xylp	BB	7.8	5.9	5.2	3.5	6.7	4.2	3.4	2.8	10.5	10.7	10.7	12.6	9.0	11.3	11.0	
Galactose <sup>b</sup> (% mol)	t-Galp	TS	2.7	3.8	3.9	4.5	3.4	6.7	7.1	7.7	2.2	4.5	2.2	3.5	4.5	2.8	7.1
Uronic <sup>c</sup> (% mol)	3-Galp	OS	1.7	1.7	2.1	2.4	1.7	1.0	1.1	1.3	2.0	1.8	0.7	1.8	0.8	1.7	0.3
GlcA	TS	5.3	5.1	5.8	6.2	5.9	5.6	5.8	5.9	3.2	8.4	9.7	10.2	14.6	11.4	3.2	11.5
m-GlcA	TS	0.1	0.2	0.2	0.2	0.0	0.2	0.2	0.2	0.0	0.2	0.2	0.0	0.0	0.5	0.1	0.1
A/X in GAX <sup>d</sup>		1.35	1.10	0.81	0.57	0.94	0.73	0.54	0.37	0.58	0.52	0.52	0.44	0.81	0.60	0.48	0.47
Average molar mass by SEC-DRI-MALLS in DMSO/LiBr																	
$M_n$ (kDa)	11.6	12.9	11.7	9.3	12.5	10.1	8.9	6.4	4.1	3.8	6.7	15.4	3.3	4.1	10.3	17.5	
$M_w$ (kDa)	367.1	105.5	57.6	32.9	211.3	61.7	32.5	18.9	182.3	155.4	178.1	225.1	145.0	163.2	199.8	195.9	
Dispersity ( $D$ )	31.6	8.2	4.9	3.5	16.9	6.1	3.6	3.0	44.0	41.3	26.5	14.6	44.6	39.7	19.3	11.2	
Acetyl content and degree of acetylation (DSAc)		—	2.7	6.0	7.7	—	1.8	3.0	3.5	—	0.7	1.5	—	0.7	0.4	1.0	
Acetyl (%)	DSAc	—	—	0.08	0.20	0.26	—	0.06	0.12	0.11	—	0.02	0.02	0.05	—	0.01	0.03

<sup>a</sup> GAX content was calculated as the sum of Xyl, Ara, Gal, GlcA and mGlcA from the monosaccharide analysis. <sup>b</sup> PMAA values were corrected to the monosaccharide content obtained from acid methanolysis and normalised to the total amount present in GAX. <sup>c</sup> The GlcA and mGlcA values (% mol) were obtained from the monosaccharide content and normalised to the total amount present in GAX. <sup>d</sup> A/X is the ratio of the sum of arabinoses present in the GAX. Note TS: terminal substitution, OS: oligomeric substitution and BB: backbone.



**Fig. 3** (a) Total solid yields and (b) extract yields from pH optimisation in the SWE. Yields are calculated in terms of percentage dry weight (% DW). (c) The pH of the extracts. Monosaccharide composition of extracts (d) and residues (e) are shown in terms of mg per gram of dry sample. The glucuronoarabinoxylan (GAX) content is estimated by the composition of xylose (Xyl), arabinose (Ara), galactose (Gal), glucuronic acid (GlcA) and 4-O-*D*-methyl glucuronic acid (mGlcA). (f) Molar mass distributions of pH optimised extracts.

luloses from biomass. In SWE, however, a much lower salt concentration is needed as opposed to traditional alkaline extraction, which simplifies downstream processing significantly. Additionally, the monosaccharide analysis showed that the

amount of galactose (Gal) and glucuronic acid (GlcA), present in GAX as side chain substitutions, increased with time. This suggests that the complexity of the substitution pattern in GAX can be controlled at different pH conditions, as it will be dis-

cussed later based on the results of glycosidic linkage analysis. Furthermore, proteins were co-extracted together with the GAX in the pH optimised extracts, as shown in ESI Table S5.† The highest amount of protein was obtained at pH 7.0, followed by pH 9.2 and pH 5.0. Here, the proteins can be of storage or structural origin and could have also been associated with the GAX in the corn fibre.<sup>6</sup>

The use of buffered conditions in the SWE, specifically neutral and alkaline conditions, resulted in noticeably longer forms of the extracted GAX (Fig. 3f). The GAX-rich extracts (>80% GAX) obtained at pH 7.0 (60 min) and pH 9.2 (30–60 min) exhibited a molar mass distribution in the range of  $10^5$  Da, which is an order of magnitude higher than that obtained in unbuffered conditions at 160 °C. The highest  $M_w$  value was obtained at 225 kDa in the 60 min extract of pH 7.0 (Table 1). Shoulder peaks were also present in the  $10^3$ – $10^4$  Da range, which likely represent shorter GAX chains and possibly glucans, which were prevalent in the 5 min extract at all pH conditions. This outcome marks the importance of mitigating pH drop in the extracts during SWE, by using buffered solutions to prevent the occurrence of autohydrolysis reactions, especially when higher molar mass of GAX is desired for material applications.

### Temperature and pH during SWE modulate the degree and pattern of substitution in extracted GAX

The molecular structure of GAX, due to its convoluted nature, is a challenging task to define. Traditionally, the arabinose to xylose ratio (A/X) has been used as a simple approximation of the degree of substitution in xylans from various biomasses. In this study, a considerable decrease in the A/X ratio was observed with longer extraction times in all of the conditions tested (ESI Tables S4 and S5†), suggesting that the extracted GAX became less substituted over time. Interestingly, this outcome greatly differed to our previous study in which we extracted arabinoxylans from wheat bran and observed the opposite trend.<sup>38</sup> To investigate the substitution pattern of the extracted GAX in more detail, linkage analysis was performed to try and understand where the arabinoses sit on the GAX. The arabinoses are present as part of the monomeric and oligomeric side chains, but also as unattached arabinoses, which is a likely case for the unbuffered extracts since they were not dialysed. The linkage analysis showed that other polysaccharides were present aside from GAX, which included glucans, xyloglucan, pectins, mannan and the glycosylation of extensin and arabinogalactan proteins (ESI Tables S7–S10†). It is crucial that constituents from other polysaccharides are excluded from the GAX analysis. However, some of the partially methylated alditol acetates (PMAAs) inevitably overlap; the arabinose detected can also come from the pectins and glycosylated portion of extensin and arabinogalactan. In principle, the glycosylation of extensin consists of  $\beta$ -(1 → 2)-linked arabinose chains with a terminal  $\alpha$ -(1 → 3) arabinosyl residue,<sup>67</sup> while the glycosylation of arabinogalactan contains  $\beta$ -(1 → 3) and  $\beta$ -(1 → 6)-linked galactose chains, linked to terminal arabinosyl residues by either an  $\alpha$ -(1 → 3) or  $\beta$ -(1 → 6) linkage.

Additionally, arabinogalactans can contain arabinose chains that are  $\beta$ -(1 → 2)-linked<sup>66–69</sup> (ESI Fig. S3†). Thus, assignment of the arabinosyl PMAAs from the linkage analysis has proven to be difficult since the t-Araf, 2-Araf and 3-Araf can originate from both these proteins and GAX (ESI Tables S7–S10†). However, due to the lower amount of PMAAs that solely originate from the arabinogalactan (6-Gal and 3,6-Gal) and the high amount of xylose that mainly correspond to the GAX backbone, we have assumed that a majority of the overlapping arabinosyl PMAAs originate from GAX.

A normalised linkage composition of the PMAAs and uronic acids with respect to GAX is shown in Table 1. In unbuffered conditions, the linkage analysis supports the notion that the GAX became less substituted over time, as shown by the clear increase of unsubstituted Xylp (4-Xylp) and the decrease of terminal Araf (t-Araf) in the 160 °C (Fig. 4a) and 180 °C extracts (Table 1). A large portion of the t-Araf are presumably unattached from the GAX, as depicted in Fig. 4d. A proposed hypothesis is that the crossed-linked GAX is first solubilised in subcritical water and once soluble, the terminal arabinosyl substitutions in the non-reducing end became prone to cleavage. Arabinosyl substitutions in the furanose form are generally labile under acidic conditions,<sup>70,71</sup> thus in the absence of a buffered environment, the drop of pH during the SWE could have contributed to their hydrolysis. In contrast, other sugars that contribute to both terminal (t-Xylp, t-Galp, GlcA) and oligomeric (2-Araf) substitutions of GAX showed a general increase with time (Fig. 4b and c). The 2-Xylp PMAA, which should be present in longer oligomeric substitutions (ESI Table S6†), was only detected in trace amounts in the linkage analysis. Such result indicates that these more complex decorations in corn GAX are more recalcitrant to extraction and require severe temperature and time conditions to be extracted.

Contrarily to the effect of unbuffered subcritical water, the use of buffered conditions at pH 7.0 and pH 9.2 preserve to a larger extent the complex substitution pattern of corn GAX during SWE. Indeed, the ratio of unsubstituted Xylp (4-Xylp) generally decreased with time, while the relative amount of substituted Xylp units in the backbone (mainly 3,4-Xylp and 2,3,4-Xylp) increased with time (Fig. 4e and Table 1). To add, the amount of t-Araf at pH 7.0 and pH 9.2 remained relatively higher in contrast to the unbuffered water. Such results further support the notion that the use of buffered neutral and mild alkaline conditions protect the labile terminal Araf substitutions covalently attached to the GAX backbone, thus mitigating their release and degradation observed under unbuffered and acidic conditions. Meanwhile, the relative content of the terminal substitutions t-Xylp and GlcA increased markedly at both pH 7.0 and pH 9.2 compared to the unbuffered conditions. The presence of oligomeric substitutions, represented by 2-Araf, also largely increased, suggesting the overall GAX structure became more complexly substituted over time (Fig. 4d).

This demonstrates that controlling the temperature, time and pH conditions during SWE enables to control not only the molar mass but also the molecular complexity and substi-



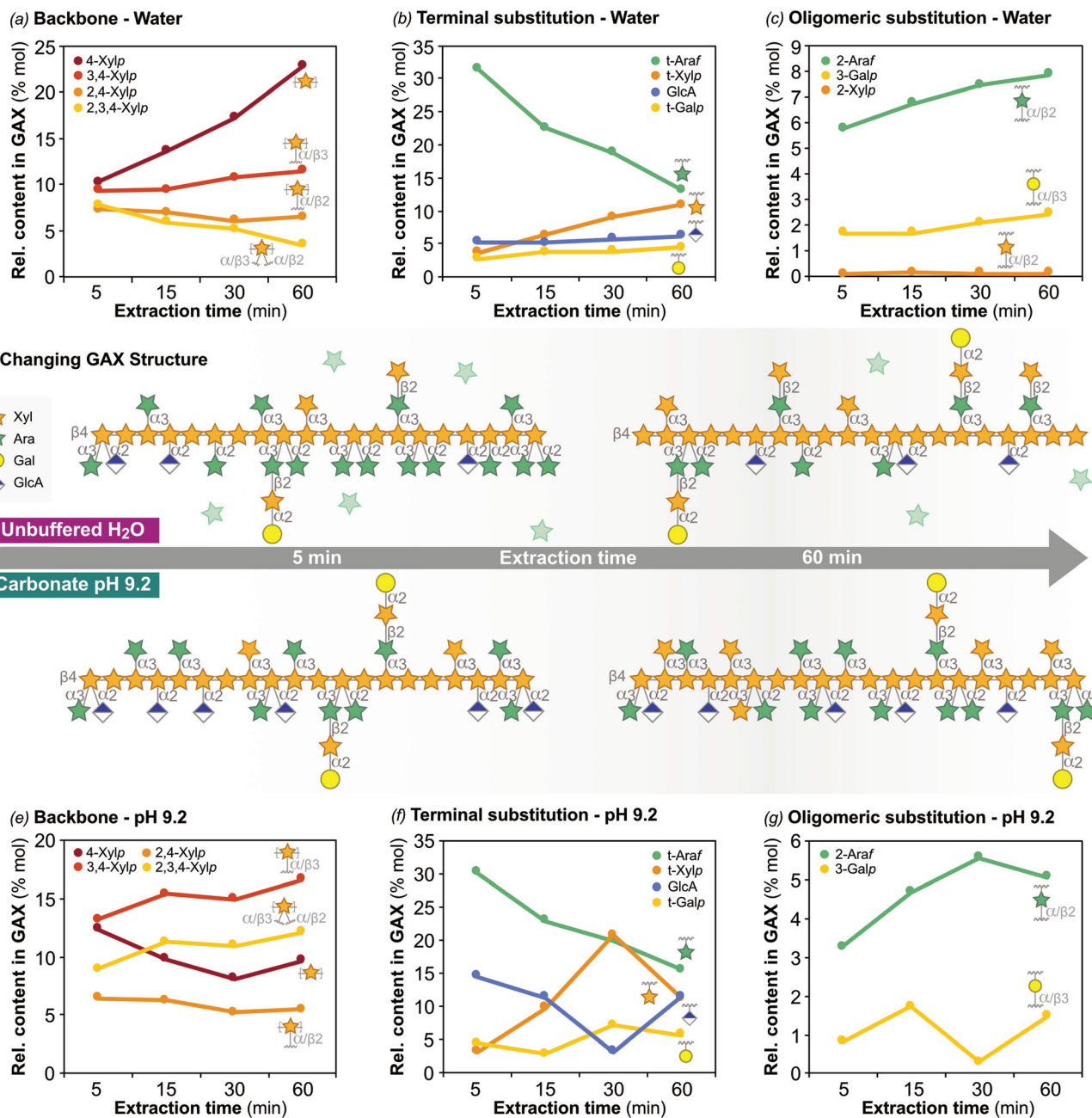


Fig. 4 Changes in the substitution of GAX as an effect of temperature and pH over time. (a) Xylan backbone, (b) terminal substitution and (c) oligomeric substitution of extracted GAX at 160 °C using unbuffered water. (d) Illustration of the GAX structures based on the linkage analysis using unbuffered water (top) and carbonate buffer at pH 9.2 (bottom) as solvents, at 5 and 60 min, respectively. Construction of the GAX structure was based on the linkage analysis and calculations can be found in the ESI.† (e) Xylan backbone, (f) terminal substitution and (g) oligomeric substitution of extracted GAX at 160 °C using carbonate buffer pH 9.2. All values correspond to the normalised linkage composition in respect to GAX.

tuation pattern of corn GAX. This has large implications for the exploitation of such complex hemicelluloses in material and food applications, for instance during microbial fermentation in the gut,<sup>72</sup> and for their enzymatic deconstruction for the production of biofuels.<sup>41</sup> Extraction of corn fibre with unbuffered water results in a more exposed xylan backbone, as considerable terminal Araf substitutions are released (Fig. 4d); however, single substitutions of Xylp and GlcA along with

longer oligomeric substitutions seem to withstand the SWE conditions. A more exposed backbone will favour the action of specific  $\beta$ -xylanases (e.g. xylanases from families GH10, 11 and 8) that are limited by complex substitutions to a certain extent.<sup>73–75</sup> From a materials perspective, the occurrence of an exposed xylan backbone with longer stretches of unsubstituted Xylp units may favour interchain interactions that are hindered by the presence of decorations, as it has been previously

reported for arabinoxylans.<sup>76</sup> On the other hand, buffered pH conditions result in a richer substitution pattern, with a larger abundance of not only the canonical t-Araf decorations, but also terminal GlcA and t-Xylp substitutions and more complex oligosaccharide side groups. From a biochemical perspective, the presence of a richer substitution will prevent the action of specific  $\beta$ -xylanases that require unsubstituted backbone towards other  $\beta$ -xylanase families (e.g. GH5 and GH30

$\beta$ -xylanases)<sup>77,78</sup> and will require a much more complex and specific enzymatic machinery involving a larger number of *exo*-acting xylanolytic enzymes for its complete deconstruction (e.g. glucuronosidases, galactosidases).<sup>41</sup> Meanwhile, from a material science perspective, the presence of a rich diversity of glycan decorations in corn GAX provides exciting new avenues for their chemo-enzymatic modification towards targeted rheological and viscoelastic properties.

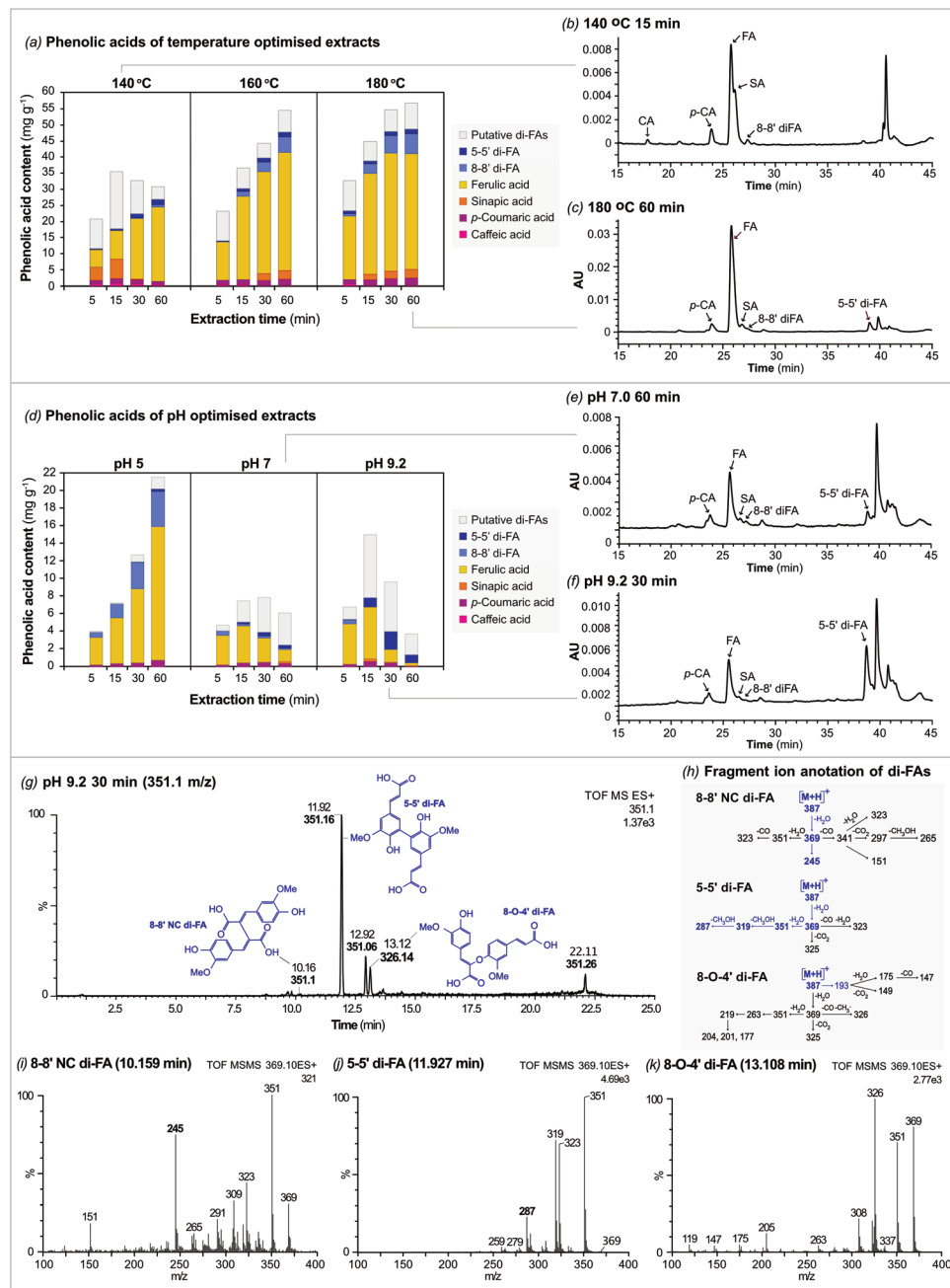


Fig. 5 (a) Phenolic acid profile of the temperature optimised extracts. HPLC chromatograms of the (a) 15 min extract at 140 °C and (b) 60 min extract at 180 °C, both at 325 nm. Note CA: caffeic acid, p-CA: *p*-coumaric acid, FA: ferulic acid, SA: Sinapic acid, 8–8' di-FA: 8–8' ferulic acid dehydrodimer 5–5' di-FA: 5–5' ferulic acid dehydrodimer. (d) Phenolic acid profile of the pH optimised extracts. HPLC chromatograms of the (e) 60 min extract at pH 7.0 and (f) 30 min extract at pH 9.2, both at 325 nm. (g) Ion extracted HPLC-ESI-MS chromatogram of the 30 min extract at pH 9.2 (351.1  $m/z$ ). (h) Fragment ion annotation of di-FA.<sup>80</sup> (i–k) CID MS<sup>2</sup> spectra of identified di-FA isomers.



## Temperature and pH conditions during SWE modulate the content and nature of the phenolic acid moieties in corn GAX with antioxidant properties

Corn GAX contains a high content of phenolic acids in comparison to other cereal grains, with ferulic acid being the most abundant form.<sup>14,18</sup> During extraction, these phenolic acids can be co-extracted with the main carbohydrate constituent of the GAX both in free form and covalently attached to the polysaccharide core (Fig. 5a and d). In the unbuffered extracts, the phenolics acids measured included both that were free and esterified to the GAX since these extracts were not dialysed. Ferulic acid was measured as the major phenolic acid present, ranging between 46.6 to 85.8% of the total phenolic acids. Its content increased steadily with time at all temperatures, in compliance with the increasing GAX content (Fig. 2d). Aside from the monomeric form, ferulic acid dehydrodimers (di-FA) were also present in the extracts. The 8-8' and 5-5' di-FAs were quantified due the presence of standards and these di-FAs clearly increased with time, especially at 160 °C and 180 °C. The enrichment of these di-FAs implies that the GAX released was possibly cross-linked and required higher temperatures and longer extraction time for release. The presence of other ferulic acid dehydrodimers, which were not quantified in the analysis, could further support this notion of cross-linking. In the HPLC chromatograms (Fig. 5b and c and ESI Fig. S4†), we observed other peaks eluting closely to the 5-5' di-FA which could presumably be other forms of di-FAs, namely the 8,5', 8-O-4' and 4-O-5' linked dehydrodimers.<sup>13</sup> In an effort to identify the unassigned peaks, the phenolic acid samples were further analysed using HPLC-ESI-MS<sup>2</sup>, revealing that indeed other di-FAs were present in the extract. Thus, to account for the presence of these putative di-FAs, we have crudely estimated their amount using the response factor of the 5-5' di-FA and collectively combined them as 'putative di-FAs'. Fig. 5a shows that the estimated amount of these putative di-FAs is quite significant, reaching up to 50% in the 15 min extract at

140 °C (Fig. 5b). Lower amounts of *p*-coumaric, sinapic and caffeic acid were also detected in the extracts.

In the buffered conditions, pH greatly affected the phenolic acid profile of the extracts. It is well known that alkaline conditions cleave off ester-linked phenolic acids that are attached to the arabinosyl units of the GAX.<sup>36</sup> Nevertheless, low amounts of phenolic acids may still remain after treatment with mild alkaline conditions.<sup>26,62,63</sup> The loss of phenolic acids is clearly shown by the low ferulic acid content of the pH 9.2 extracts (Fig. 4d). When GAX content was highest, *i.e.* at 30 and 60 min (Fig. 3d), the ferulic acid content was in fact lowest, at 1.4 and 0.3 mg g<sup>-1</sup>, respectively. Surprisingly, the 5-5' di-FA along with the putative di-FAs were particularly enriched in the pH 9.2 extracts. This implies that the di-FAs could withstand the alkaline condition in the SWE and remained linked to the GAX, as these extracts underwent dialysis. The high abundance of the di-FAs also suggests that the GAX extracted at pH 9.2 are particularly complex, possibly being cross-linked to each other (Fig. 3f and Table 2).<sup>79</sup> Meanwhile at pH 5.0, the ferulic acid was preserved along with the 8-8' diFA and their content progressively increased with increasing GAX content (Fig. 3d and Table 2). At pH 7.0, monomeric ferulic acid decreased with time, while the opposite trend occurred for the di-FAs.

To confirm the presence of other di-FAs being present aside from the 8-8' and 5-5' di-FAs, HPLC-ESI-MS<sup>2</sup> was performed on the saponified samples. In the chromatograms, we observed peaks that exhibited mass to charge ratios of mainly 369 *m/z* and 351 *m/z*, which corresponded to dehydrated di-FAs in adduct with a proton, [M - H<sub>2</sub>O + H]<sup>+</sup> and [M - 2H<sub>2</sub>O + H]<sup>+</sup>, respectively. Several peaks, from the 30 min extract of pH 9.2, were observed in the initial and ion extracted chromatograms (ESI Fig. S7† and Fig. 4g). The 369 *m/z* ion was subjected to CID-MS<sup>2</sup> and the resulting spectra was annotated according to a previously reported MS<sup>2</sup> spectra,<sup>80</sup> as shown in Fig. 5h. The MS<sup>2</sup> spectra revealed that indeed the sample contained several different forms of di-FA isomers (Fig. 5i-k). The 30 min

**Table 2** Phenolic acid content and radical scavenging activity of extracted GAX

	Temperature optimisation								pH optimisation							
	160 °C				180 °C				pH 7.0				pH 9.2			
	5'	15'	30'	60'	5'	15'	30'	60'	5'	15'	30'	60'	5'	15'	30'	60'
Phenolic acid content after saponification																
Phenolic acid <sup>a</sup> (mg g <sup>-1</sup> DW)	14.1	30.3	39.7	47.8	23.4	38.9	47.9	48.7	4.0	5.1	3.9	2.4	5.4	7.8	3.9	1.4
Caffeic acid (%)	3.3	1.5	0.6	0.4	2.2	0.8	0.5	0.6	0.0	0.0	0.0	0.0	0.0	0.0	0.0	0.0
<i>p</i> -Coumaric acid (%)	8.9	4.8	3.7	3.8	6.2	4.1	4.2	4.6	4.5	8.8	11.9	15.5	5.4	7.5	10.5	3.6
Ferulic acid (%)	84.9	85.7	79.6	76.8	84.5	80.6	76.8	73.6	83.1	80.9	69.7	54.5	84.7	74.0	35.7	21.1
Sinapic acid (%)	0.0	0.0	5.3	5.5	0.0	4.5	4.8	5.5	0.0	0.0	2.2	8.4	0.0	4.2	2.8	4.6
8-8' di-FA (%)	2.1	3.0	3.1	3.1	3.8	2.7	2.5	3.0	11.6	5.7	4.8	6.2	8.5	0.0	1.0	3.5
5-5' di-FA (%)	0.7	5.0	7.7	10.3	3.3	7.3	11.3	12.7	0.9	4.7	11.3	15.3	1.4	14.4	50.0	67.2
Radical scavenging activity against DPPH																
EC <sub>50</sub> <sup>b</sup> (mg mg <sup>-1</sup> DPPH)	5.8	5.3	4.6	4.2	4.9	4.4	3.9	3.9	10.4	7.2	6.1	6.2	10.1	3.3	4.9	6.8

<sup>a</sup> Phenolic acid content was determined by saponification followed by HPLC analysis. <sup>b</sup> EC<sub>50</sub> is the effective concentration that resulted in 50% of DPPH scavenging activity.

extract of pH 9.2 contained the 8–8' non-cyclic di-FA (10.2 min) as confirmed by the standard and further distinguished by the 245  $m/z$  ion. It also contained the 5–5' di-FA that eluted at both 11.9 min and 12.9 min as confirmed by the standard (ESI Fig. S6†) and identified by the 287  $m/z$  and 319  $m/z$  ions. Another di-FA (eluting at 13.1 min) was presumably assigned as the 8-O-4' di-FA, owing to the recalcitrance of the 369  $m/z$  ion to fragmentation and the high abundance of the 326  $m/z$  ion.<sup>80</sup> Such result complies with previous studies highlighting that the most abundant di-FAs present in corn are the 8-O-4', 5–5', 8–8' and 8–5',<sup>13,66</sup> although the 8–5' di-FA was not detected in this particular sample.

The preservation of these phenolic moieties is of great importance, mainly for the fabrication of enzyme-assisted hydrogels *via* oxidative coupling<sup>25,26</sup> and also for their anti-oxidant activity. Here, we tested the scavenging activity of the GAX extracts against the radical 2,2-diphenyl-1-picrylhydrazyl (DPPH), as shown in Table 2. All the extracts exhibited radical scavenging activity and the highest activity was provided by the 30 min and 60 min extracts of 180 °C, whereby the phenolic acid content was also highest at 47.9 and 48.7 mg g<sup>-1</sup>. The correlation between the phenolic acid concentration and overall scavenging activity is, however, non-linear as each individual phenolic acid has a different capability to scavenge DPPH.<sup>81</sup> Interestingly, the pH 9.2 extracts, which have lost a large portion of their phenolic acids, still exhibited comparable scavenging activities compared to other extracts. This was most likely attributed to the unanticipated presence of di-FAs (5–5' diFA, 8–8' diFA and other putative di-FAs).

## Conclusions

We propose an integral process by aqueous steeping and sub-critical water extraction to fractionate the polysaccharide components (*e.g.* starch and GAX) from corn fibre, a large by-product from the corn milling industry. Starch can be fully recovered in intact form, whereas subsequent SWE enables the extraction of recalcitrant GAX in polymeric form with preserved glycosyl motifs and phenolic acid functionalities. Furthermore, controlling the critical operating parameters (temperature, pH and time) during SWE greatly influence the performance of extraction in terms of yields and purity, as well as the molecular structure of the extracted GAX. Higher temperatures in unbuffered conditions favour extraction yields and purities but at the expense of lower molar masses of the GAX; this is caused by a sharper drop in pH due to deacetylation, resulting in autohydrolysis and the release of arabinose substitutions. Contrarily, the use of buffered neutral and alkaline conditions in SWE preserved a high molar mass as well as the complex monomeric and oligomeric substitution patterns present in GAX. Alkaline conditions also resulted in high extraction yields and purities of the GAX, however, at the cost of a lower phenolic acid content. Unexpectedly, di-FAs were enriched in the alkaline extracts, highlighting their perseverance towards cleavage during extraction. Preservation of phe-

nolic acids adds value to the GAX by providing radical scavenging activity and the possibility to engineer crossed-linked materials, *i.e.* hydrogels. The specific combination of temperature, pH and time in SWE can be used to effectively tune the molar mass and complex substitution pattern of GAX from corn fibre without the use of additional catalysts. As application development is highly reliant on the GAX structure, our process has large implications for the potential use of corn GAX in material and food applications, for instance in the modulation of the gut microbiota in nutritional prebiotic applications, as well as in the enzymatic deconstruction prior to fermentation processes, both for the production of biofuels and platform chemicals. Our SWE approach therefore offers an efficient and eco-friendly mode of GAX production, which can hopefully benefit the future realisation of agroindustry-based biorefineries.

## Conflicts of interest

There are no conflicts to declare.

## Acknowledgements

The authors acknowledge the financial support to the project BARBARA – Biopolymers with advanced functionalities for building and automotive parts processed through additive manufacturing. This project has received funding from the Bio Based Industries Joint Undertaking under the European Union's Horizon 2020 research and innovation programme under grant agreement no. 745578.

## References

- 1 F. Cherubini and S. Ulgiati, *Appl. Energy*, 2010, **87**, 47–57.
- 2 FAO, Crops, <http://www.fao.org/faostat/en/#data/QC/visualize>, (accessed[:]) August 3, 2020).
- 3 E. C. Ramirez, D. B. Johnston, A. J. McAloon, W. Yee and V. Singh, *Ind. Crops Prod.*, 2008, **27**, 91–97.
- 4 M. Gáspár, G. Kálmán and K. Réczey, *Process Biochem.*, 2007, **42**, 1135–1139.
- 5 J. A. Gwirtz and M. N. Garcia-Casal, *Ann. N. Y. Acad. Sci.*, 2014, **13121**, 66–75.
- 6 E. Chanliaud, L. Saulnier and J.-F. Thibault, *J. Cereal Sci.*, 1995, **21**, 195–203.
- 7 M. Gáspár, T. Juhász, Z. Szengyel and K. Réczey, *Process Biochem.*, 2005, **40**, 1183–1188.
- 8 M. M. H. Huisman, H. A. Schols and A. G. J. Voragen, *Carbohydr. Polym.*, 2000, **44**, 269–279.
- 9 G. B. Fincher and B. A. Stone, in *Encyclopedia of Grain Science*, ed. C. Wrigley, H. Corke and C. E. Walker, Elsevier, Oxford, 2004, pp. 206–223.
- 10 L. Saulnier, C. Marot, E. Chanliaud and J.-F. Thibault, *Carbohydr. Polym.*, 1995, **26**, 279–287.



11 E. Allerdings, H. Steinhart and M. Bunzel, *Phytochemistry*, 2006, **67**, 1276–1286.

12 M. M. Appeldoorn, P. D. Waard, M. A. Kabel, H. Gruppen and H. A. Schols, *Carbohydr. Res.*, 2013, **381**, 33–42.

13 A. Bento-Silva, M. C. Vaz Patto and M. D. R. Bronze, *Food Chem.*, 2018, **246**, 360–378.

14 P. Vitaglione, A. Napolitano and V. Fogliano, *Trends Food Sci. Technol.*, 2008, **19**, 451–463.

15 A.-L. Chateigner-Boutin, J. J. Ordaz-Ortiz, C. Alvarado, B. Bouchet, S. Durand, Y. Verhertbrugge, Y. Barrière and L. Saulnier, *Front. Plant Sci.*, 2016, **7**, 1476.

16 L. Saulnier, J. Vigouroux and J.-F. Thibault, *Carbohydr. Res.*, 1995, **272**, 241–253.

17 C. Lapierre, B. Pollet, M.-C. Ralet and L. Saulnier, *Phytochemistry*, 2001, **57**, 765–772.

18 L. Saulnier and J.-F. Thibault, *J. Sci. Food Agric.*, 1999, **79**, 396–402.

19 R. R. Schendel, M. R. Meyer and M. Bunzel, *Front. Plant Sci.*, 2016, **6**, 1249.

20 B. R. Hamaker, Y. E. Tuncil and X. Shen, in *Corn*, ed. S. O. S. Saldívar, AACC International Press, 3rd edn, 2019.

21 A. Riviere, M. Selak, D. Lantin, F. Leroy and L. De Vuyst, *Front. Microbiol.*, 2016, **7**, 1–21.

22 X. Zhang, T. Chen, J. Lim, J. Xie, B. Zhang, T. Yao and B. R. Hamaker, *Food Funct.*, 2019, **10**, 4497–4504.

23 J. Lappi, M. Kolehmainen, H. Mykkänen and K. Poutanen, *Crit. Rev. Food Sci. Nutr.*, 2013, **53**, 631–640.

24 G. Niño-Medina, E. Carvajal-Millán, J. Lizardi, A. Rascon-Chu, J. A. Marquez-Escalante, A. Gardea, A. L. Martinez-Lopez and V. Guerrero, *Food Chem.*, 2009, **115**, 1286–1290.

25 X. Zhang, T. Chen, J. Lim, F. Gu, F. Fang, L. Cheng, O. H. Campanella and B. R. Hamaker, *Food Hydrocolloids*, 2019, **92**, 1–9.

26 M. S. Kale, B. Hamaker and O. Campanella, *Food Hydrocolloids*, 2013, **31**, 121–126.

27 M. A. Mendez-Encinas, E. Carvajal-Millan, A. Rascon-Chu, H. F. Astiazaran-Garcia and D. E. Valencia-Rivera, *Oxid. Med. Cell. Longevity*, 2018, **2018**, 1–23.

28 H. Gruppen, R. J. Hamer and A. G. J. Voragen, *J. Cereal Sci.*, 1991, **13**, 275–290.

29 M. G. Jackson, *Anim. Feed Sci. Technol.*, 1977, **2**, 105–130.

30 M. Cyran, C. M. Courtin and J. A. Delcour, *J. Agric. Food Chem.*, 2004, **52**, 2671–2680.

31 A. Ghaffar, M. Yameen, N. Aslam, F. Jalal, R. Noreen, B. Munir, Z. Mahmood, S. Saleem, N. Rafiq, S. Falak, I. Tahir, M. Noman, M. Farooq, S. Qasim and F. Latif, *Chem. Cent. J.*, 2017, **11**, 1–6.

32 F. Xu, C. F. Liu, Z. C. Geng, J. X. Sun, R. C. Sun, B. H. Hei, L. Lin, S. B. Wu and J. Je, *Polym. Degrad. Stab.*, 2006, **91**, 1880–1886.

33 A. A. Peterson, F. Vogel, R. P. Lachance, M. Fröling, J. M. J. Antal and J. W. Tester, *Energy Environ. Sci.*, 2008, **1**, 32–65.

34 Z. M. Alghoul, P. B. Ogden and J. G. Dorsey, *J. Chromatogr. A*, 2017, **1486**, 42–49.

35 A. Mustafa and C. Turner, *Anal. Chim. Acta*, 2011, **703**, 8–18.

36 A. C. Ruthes, A. Martinez-Abad, H.-T. Tan, V. Bulone and F. Vilaplana, *Green Chem.*, 2017, **19**, 1919–1931.

37 A. C. Ruthes, R. C. Rudjito, J. Rencoret, A. Gutierrez, J. C. del Río, A. Jiménez-Quero and F. Vilaplana, *ACS Sustainable Chem. Eng.*, 2020, **8**, 7192–7204.

38 R. C. Rudjito, A. C. Ruthes, A. Jimenez-Quero and F. Vilaplana, *ACS Sustainable Chem. Eng.*, 2019, **7**, 13167–13177.

39 F. Bertaude, A. Sundberg and B. Holmbom, *Carbohydr. Polym.*, 2002, **48**, 319–324.

40 J. F. M. Saeman, E. Wayne, R. L. Mitchell and M. A. Millett, *Tappi J.*, 1954, **37**, 336–343.

41 L. S. McKee, H. Sunner, G. E. Anasontzis, G. Toriz, P. Gatenholm, V. Bulone, F. Vilaplana and L. Olsson, *Biotechnol. Biofuels*, 2016, **9**, 1–13.

42 F. Vilaplana, J. Hasjim and R. G. Gilbert, *Carbohydr. Polym.*, 2012, **88**, 103–111.

43 C. Antoine, S. Peyron, F. Mabille, C. Lapierre, B. Bouchet, J. Abecassis and X. Rouau, *J. Agric. Food Chem.*, 2003, **51**, 2026–2033.

44 P. Comino, H. Collins, J. Lahnstein, C. Beahan and M. J. Gidley, *Food Hydrocolloids*, 2014, **41**, 219–226.

45 A. Martínez-Abad, N. Giummarella, M. Lawoko and F. Vilaplana, *Green Chem.*, 2018, **20**, 2534–2546.

46 M. M. Bradford, *Anal. Biochem.*, 1976, **72**, 248–254.

47 W. Brand-Williams, M. E. Cuvelier and C. Berset, *LWT-Food Sci. Technol.*, 1995, **28**, 25–30.

48 F. A. Pettolino, C. Walsh, G. B. Fincher and A. Bacic, *Nat. Protoc.*, 2012, **7**, 1590.

49 B. Imre and F. Vilaplana, *Green Chem.*, 2020, **22**, 5017–5031.

50 B. Imre, L. García, D. Puglia and F. Vilaplana, *Carbohydr. Polym.*, 2019, **209**, 20–37.

51 M. J. Cocero, Á. Cabeza, N. Abad, T. Adamovic, L. Vaquerizo, C. M. Martínez and M. V. Pazo-Cepeda, *J. Supercrit. Fluids*, 2018, **133**, 550–565.

52 X. Chen, M. Lawoko and A. V. Heiningen, *Bioresour. Technol.*, 2010, **101**, 7812–7819.

53 J. V. Rissanen, H. Grénman, C. Xu, J. Krogell, S. Willför, D. Y. Murzin and T. Salmi, *Cellul. Chem. Technol.*, 2015, **49**, 449–453.

54 D. Macdonald, S. Hettiarachchi, H. Song, K. Makela, R. Emerson and M. Ben-Haim, *J. Solution Chem.*, 1992, **21**, 849–881.

55 G. Garrote, H. Domínguez and J. C. Parajó, *Eur. J. Wood Wood Ind.*, 2001, **59**, 53–59.

56 L. Michalak, S. Knutsen, I. Aarum and B. Westereng, *Biotechnol. Biofuels*, 2018, **11**, 1–12.

57 G. Gallina, E. R. Alfageme, P. Biasi and J. García-Serna, *Bioresour. Technol.*, 2018, **247**, 980–991.

58 J. Rissanen, H. Grenman, S. Willfor, D. Murzin and T. Salmi, *Ind. Eng. Chem. Res.*, 2014, **53**, 6341–6350.

59 H. Chen, in *Lignocellulose Biorefinery Feedstock Engineering*, ed. C. Hongzhang, Elsevier, 2015, ch 3, pp. 37–86.

60 N. P. Nghiem, J. Montanti, D. B. Johnston and C. Drapcho, *Appl. Biochem. Biotechnol.*, 2011, **164**, 1390–1404.

61 B. C. Saha, *J. Ind. Microbiol. Biotechnol.*, 2003, **30**, 279–291.

62 M. P. Yadav, M. L. Fishman, H. K. Chau, D. B. Johnston and K. B. Hicks, *Cereal Chem.*, 2007, **84**, 175–180.

63 M. P. Yadav, D. B. Johnston, A. T. Hotchkiss and K. B. Hicks, *Food Hydrocolloids*, 2007, **21**, 1022–1030.

64 S. García-Lara, C. Chuck-Hernandez and S. O. Serna-Saldivar, in *Corn*, ed. S. O. Serna-Saldivar, AACC International Press, 3rd edn, 2019, ch. 6, pp. 147–163.

65 J. W. Lawton, *Cereal Chem.*, 2002, **79**, 1–18.

66 J. Agger, PhD thesis, Technical University of Denmark, 2011.

67 S. C. Fry, *The growing plant cell wall: chemical and metanolic analysis*, Wiley, New York, 1988.

68 A. M. Showalter, *Cell. Mol. Life Sci.*, 2001, **58**, 1399–1417.

69 J. Sommer-Knudsen, A. Bacic and A. E. Clarke, *Phytochemistry*, 1998, **47**, 483–497.

70 R. L. Whistler and W. M. Corbett, *J. Am. Chem. Soc.*, 1955, **77**, 6328–6330.

71 K. Grohmann and R. J. Bothast, *Process Biochem.*, 1997, **32**, 405–415.

72 A. Rogowski, J. A. Briggs, J. C. Mortimer, T. Tryfona, N. Terrapon, E. C. Lowe, A. Baslé, C. Morland, A. M. Day, H. Zheng, T. E. Rogers, P. Thompson, A. R. Hawkins, M. P. Yadav, B. Henrissat, E. C. Martens, P. Dupree, H. J. Gilbert and D. N. Bolam, *Nat. Commun.*, 2015, **6**, 7481.

73 M. Vardakou, C. Dumon, J. W. Murray, P. Christakopoulos, D. P. Weiner, N. Juge, R. J. Lewis, H. J. Gilbert and J. E. Flint, *J. Mol. Biol.*, 2008, **375**, 1293–1305.

74 G. Pell, E. J. Taylor, T. M. Gloster, J. P. Turkenburg, C. M. G. A. Fontes, L. M. A. Ferreira, T. Nagy, S. J. Clark, G. J. Davies and H. J. Gilbert, *J. Biol. Chem.*, 2004, **279**, 9597–9605.

75 A. Pollet, J. A. Delcour and C. M. Courtin, *Crit. Rev. Biotechnol.*, 2010, **30**, 176–191.

76 A. Höije, E. Stememalm, S. Heikkinen, M. Tenkanen and P. Gatenholm, *Biomacromolecules*, 2008, **9**, 2042–2047.

77 M. A. S. Correia, K. Mazumder, J. L. A. Brás, S. J. Firbank, Y. Zhu, R. J. Lewis, W. S. York, C. M. G. A. Fontes and H. J. Gilbert, *J. Biol. Chem.*, 2011, **286**, 22510–22520.

78 E. N. Karlsson, E. Schmitz, J. A. Linares-Pastén and P. Adlercreutz, *Appl. Microbiol. Biotechnol.*, 2018, **102**, 9081–9088.

79 G. Derville, L. Saulnier, P. Roger and J. Thibault, *J. Agric. Food Chem.*, 2000, **48**, 270.

80 R. Vismeh, F. Lu, S. P. S. Chundawat, J. F. Humpula, A. Azarpira, V. Balan, B. E. Dale, J. Ralph and A. D. Jones, *Analyst*, 2013, **138**, 6683–6692.

81 H. Kikuzaki, M. Hisamoto, K. Hirose, K. Akiyama and H. Taniguchi, *J. Agric. Food Chem.*, 2002, **50**, 2161–2168.

